Available online at www.sciencedirect.com
ScienceDirect
Journal of Power Sources 166 (2007) 120–126
JOURNAL OF POWER SOURCES
www.elsevier.com/locate/jpowsour

A direct-flame solid oxide fuel cell (DFFC) operated on methane, propane, and butane

Helmut Kronemayer [a], Daniel Barzan [b], Michio Horiuchi [c], Shigeaki Suganuma [c], Yasue Tokutake [c], Christof Schulz [a], Wolfgang G. Bessler [b,*]

[a] *Institut für Verbrennung und Gasdynamik (IVG), Universität Duisburg-Essen, Lotharstrasse 1, 47057 Duisburg, Germany*
[b] *Interdisciplinary Center for Scientific Computing (IWR), Universität Heidelberg, Im Neuenheimer Feld 368, 69120 Heidelberg, Germany*
[c] *Shinko Electric Industries, Nagano 381-0014, Japan*

Received 28 September 2006; received in revised form 19 December 2006; accepted 28 December 2006
Available online 13 January 2007

Abstract

This paper presents an experimental study of a direct-flame type solid oxide fuel cell (DFFC). The operation principle of this system is based on the combination of a combustion flame with a solid oxide fuel cell (SOFC) in a simple, no-chamber setup. The flame front serves as fuel reformer located a few millimeters from the anode surface while at the same time providing the heat required for SOFC operation. Experiments were performed using 13-mm-diameter planar SOFCs with Ni-based anode, samaria-doped ceria electrolyte and cobaltite cathode. At the anode, a 45-mm-diameter flat-flame burner provided radially homogeneous methane/air, propane/air, and butane/air rich premixed flames. The cell performance reaches power densities of up to 120 mW cm^{-2}, varying systematically with flame conditions. It shows a strong dependence on cell temperature. From thermodynamic calculations, both H_2 and CO were identified as species that are available as fuel for the SOFC. The results demonstrate the potential of this system for fuel-flexible power generation using a simple setup.

Keywords: Direct-flame solid oxide fuel cell; DFFC; SOFC; Hydrocarbon; Reforming; Partial oxidation

1. Introduction

The operation principle of a direct-flame solid oxide fuel cell (DFFC) is based on the combination of a combustion flame with a solid oxide fuel cell (SOFC) in a simple, "no-chamber" setup [1] illustrated in Fig. 1. In this system, a fuel-rich flame is placed at few millimeters from the anode. It serves as partial oxidation reformer while at the same time providing the heat required for SOFC operation. The cathode is freely exposed to ambient air. Flame and fuel cell are geometrically and electrochemically coupled.

There are a number of advantages to this approach. First, the system is very fuel-flexible. Because intermediate flame species are similar for all kinds of hydrocarbons, the DFFC can be operated on virtually any carbon-based fuel, as well as other fuels that contain hydrogen. Horiuchi et al. demonstrated electrochemical power generation using various gaseous (methane, ethane, propane, and *n*-butane), liquid (ethanol, butanol, and kerosine), and solid (paraffine wax and wood) fuels [1–3]. Second, the DFFC is operated in a very simple, no-chamber setup. The anode is simply held into the exhaust gases close to a fuel-rich flame. The cathode breathes ambient air. The system is thermally self-sustained, and there are no high-temperature sealing issues. Third, the system is started up rapidly (i.e., within seconds). The flame heat release brings the fuel cell rapidly to its operation temperature, and there is no external heater required for start-up. These features make the DFFC an attractive system for energy conversion, in particular for combined heat and power applications.

There are also a number of drawbacks associated with the DFFC type setup. This includes the relatively low overall electrical efficiency. An inherent property of the DFFC is that a part of the fuel's chemical energy is consumed in the combustion reaction and is therefore not available to electrical power

* Corresponding author. Tel.: +49 6221 548252; fax: +49 6221 548884.
E-mail address: bessler@iwr.uni-heidelberg.de (W.G. Bessler).

0378-7753/$ – see front matter © 2007 Elsevier B.V. All rights reserved.
doi:10.1016/j.jpowsour.2006.12.074

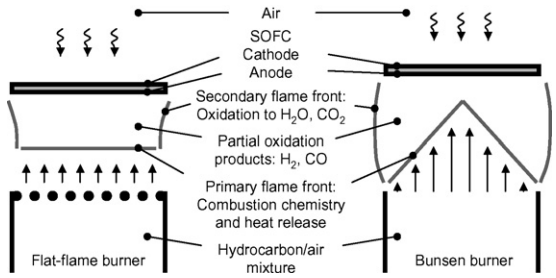

Fig. 1. Operation principle of a direct-flame solid oxide fuel cell (DFFC). *Left*: Flat-flame burner; *Right*: Bunsen-type burner.

generation. Furthermore, materials stresses are a particular challenge. The operating environment of a combustion flame can induce significant thermal stress to the SOFC.

The DFFC concept is somewhat familiar to the single-chamber solid oxide fuel cell (SCFC) concept. In the latter, the same premixed fuel/air mixture is supplied to both anode and cathode [4–7], and electrochemical fuel oxidation and oxygen reduction is achieved through selective (electro-) catalysts. Within the anode, an H_2/CO-rich atmosphere is formed via heterogeneous fuel partial oxidation reactions [8]. In the DFFC, although the setup is even simpler, the two electrodes see different gas atmospheres. The fuel is partially oxidized by homogeneous combustion flame chemistry several millimeters in front of the anode, while the cathode breathes ambient air. This setup relaxes the catalyst selectivity requirement needed for SCFCs and can therefore operated at higher temperature; it also allows higher concentrations of H_2/CO at the anode and O_2 at the cathode. Thus, the DFFC system potentially yields increased performance and efficiency. Furthermore, it does not require an external heater for the start-up phase. Finally, because partial oxidation takes place in the gas-phase instead of inside the porous electrodes, the coking problems associated with higher hydrocarbons are significantly reduced in the DFFC compared to the SCFC concept.

The idea of using rich flames for the production of synthesis gas via partial oxidation is not new. The approach has been demonstrated by several authors, in particular with the help of porous combustors [9–11]. Kendall et al. have presented a tubular SOFC with an integrated catalytic partial oxidation catalyst operated on methane and butane [12,13]. To the best of our knowledge, the use of a free flame to operate a solid oxide fuel cell was first published by Horiuchi et al. [1,2] who demonstrated the feasibility of power generation using a DFFC with a Bunsen-type burner.

In this study, we present an extended experimental analysis of DFFC performance operated on methane, propane, and *n*-butane. The experiments are carried out with a flat-flame type burner in order to match the geometries of the flame and the planar fuel cell (cf. Fig. 1). Flame operating conditions, such as equivalence ratio, fuel inflow velocity, and distance between burner and SOFC are varied in order to investigate the influence of these parameters on SOFC performance.

2. Experiment

2.1. Cell preparation

A samarium-doped ceria ($Ce_{0.8}Sm_{0.2}O_{2-\delta}$, SDC, approximately 0.2 mm) disc fired at 1300 °C for 5 h in air was prepared as an electrolyte. Cathode and anode pastes, respectively, composed of 50 wt% SDC (NexTech materials)–50 wt% samarium strontium cobaltite ($Sm_{0.5}Sr_{0.5}CoO_3$, NexTech materials), and 5 wt% Rh_2O_3–57 wt% Li (8 mol%)-doped NiO–38 wt% SDC were printed on each side of the SDC disc. Platinum wire-attached platinum meshes as electron collector were embedded in the paste layers of both sides, followed by firing in air at 1200 °C for 1 h. Diameters of both electrodes were identically 13 mm.

2.2. Flat-flame burner

For the present study, a so-called flat-flame burner was used (Fig. 1). This kind of burner applies a gas outlet that yields homogeneous gas outflow velocities over the whole area of the burner. Here, this is realized using a porous bronze sinter matrix, but a bundle of small parallel tubes or a plate with small holes would be equally suitable. The resulting combustion flame front is parallel to the burner outlet. This geometry is well-suited for direct coupling to a planar fuel cell. Furthermore, because characteristic parameters such as species concentrations and temperature in the center region of the burner only show axial, but no radial variation, this setup can be numerically studied using a one-dimensional stagnation point flow model [3,14]. This allows to calculate species concentrations in the gas-phase at the DFFC anode surface [3]. In contrast, a Bunsen-type burner as used e.g. in [1] consists of an open outlet tube, yielding a non-uniform axial velocity distribution and resulting in a typical cone-shaped flame structure (Fig. 1).

The flat-flame burner applied here uses a water-cooled (room temperature) sinter matrix of 45 mm diameter. It was operated with laminar premixed methane/air, propane/air or butane/air flames on various equivalence ratios ϕ,

$$\phi = \frac{n_{\text{fuel}}/n_{\text{air}}}{n_{\text{fuel}}^{\text{stoich}}/n_{\text{air}}^{\text{stoich}}} \quad (1)$$

where n is the molar flow rate and n^{stoich} are the flow rates needed for stoichiometric reaction. Values of $\phi > 1$ represent fuel-rich flames (oxygen deficient), values of $\phi = 1.0$ represents stoichiometric flames, and values of $\phi < 1.0$ represent fuel-lean (oxygen excess) conditions [15]. The premixed gases (methane, propane, *n*-butane, and air) were supplied using digital mass flow controllers (Bronkhorst). The flow rates were adjusted to yield the desired equivalence ratio and gas outflow velocity at the burner exit, v. The burner was mounted to a height-adjustable stage with a height resolution of 0.5 mm that allowed to conduct experiments with variable distances d between the SOFC and the burner matrix.

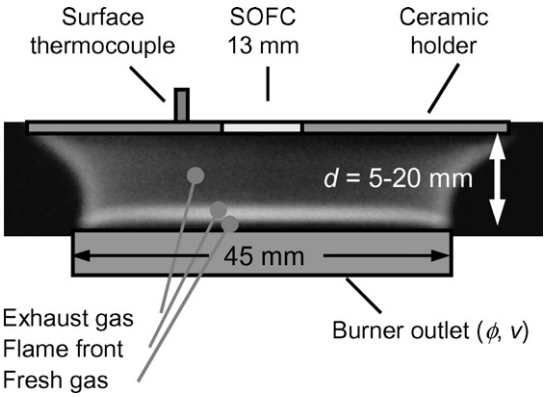

Fig. 2. Experimental setup.

A schematic of the setup is shown in Fig. 2. This figure shows clearly the flat-flame front (flame luminosity region parallel to the burner outlet). The burner flame is larger than the SOFC (13 mm diameter) in order to provide homogeneous temperature and gas composition over the complete SOFC area. This setup thus allows electrochemical characterization under defined operating conditions. The region upstream of the flame front (between burner outlet and flame front) is the fresh gas region, and the region downstream of the flame front (between the flame front and the SOFC) is the flame exhaust gas region which is, for fuel-rich premixed flames, a mixture mainly of CO_2, H_2O, CO, and H_2. The flame front itself is only a fraction of a mm thick [15]. When operating the burner with rich fuel/air mixtures as shown in Fig. 2 and throughout this paper, a secondary flame front is visible at the edges of the burner, where the H_2/CO-rich exhaust gases are fully oxidized with ambient air.

2.3. Electrochemical characterization

The SOFC was centered in the middle of the flame with the anode facing the flame. A 100-mm-diameter ceramic disc with a central hole of 13 mm diameter was used as holder for the SOFC. The SOFC was glued to the disc with the aid of a high-temperature stable ceramic glue (Kerathin K 1800). This setup is completely gas-tight. It was used in the present study to avoid convection or diffusion of flame gases from the large-diameter burner to the cathode side. In a commercial DFFC system, fuel cell and burner size would be matched so that a holder is not required.

The temperature of the upper ceramic disc surface was measured by a surface thermocouple (NiCrNi, Conrad Electronics) right next to the SOFC. The temperature at the disc surface was found to be only slightly lower (ca. 40 °C) than the temperature measured directly at the cathode surface of the SOFC. An automated test facility (Basytec) was used to acquire polarization curves. A single polarization curve measurement was acquired during ∼100 s. This slow acquisition was performed in order to give the dynamic processes at the SOFC electrodes enough time to adjust to steady-state while changing the working current.

3. Results and discussion

3.1. Polarization curves

Premixed methane/air, propane/air, and butane/air flames were investigated over a wide range of equivalence ratios ($\phi = 1.0$–1.9), gas inflow velocities ($v = 10$–$30\,\mathrm{cm\,s^{-1}}$), and distances between burner and SOFC ($d = 5$–20 mm). For each condition, a current/voltage curve and the cathode surface temperature were recorded. It was generally observed that for stoichiometric or lean flames ($\phi \leq 1.0$) the SOFC did not yield any power output (open circuit voltage = 0 V). Electrical power could be drawn only for rich flames ($\phi > 1.0$). Consequently, in the following, only results for $\phi > 1.0$ are shown.

Typical current/voltage curves are shown in Fig. 3 for methane/air flames for varying ϕ and d at $v = 20\,\mathrm{cm\,s^{-1}}$. The open circuit voltage is around 0.8–0.9 V, which is a typical value for the mixed ionic-electronic conducting electrolyte (SDC) used here where the electronic current leads to a short-circuiting of the SOFC and reduces the cell voltage [8,16]. The current/voltage curve is almost linear, with a typical maximum current density of $\sim 400\,\mathrm{mA\,cm^{-2}}$ and a maximum power density of $80\,\mathrm{mW\,cm^{-2}}$ at a cell voltage of 400 mV.

In the following, the experimental results are discussed in terms of the maximum power density that could be reached in each case.

3.2. Influence of flame conditions on the maximum power density

The maximum power density for all methane/air flames is plotted versus ϕ, v, and d in Fig. 4. The general trend that is observed is an increase in power density with increasing ϕ, increasing v, and decreasing d. However, there is some scatter, in particular at high ϕ, high v, and low d, so that a simple maximization of ϕ and v and minimization of d do not lead to the highest performance. The apparently missing data points are conditions where the flame was either unstable or could not be lighted at all.

For propane/air flames, the maximum power output is plotted versus ϕ, v, and d in Fig. 5. Here, the power density generally increases with increasing v and decreasing d. The plots of the power density versus ϕ reveal that there is a maximum equivalence ratio in the range of 1.3–1.5, with decreasing power density towards both leaner and richer flames. There is generally less scatter in the data compared to methane flames, as the flames were in general more stable in the extreme ranges of v and d.

For butane/air flames, the maximum power output is plotted versus ϕ, v, and d in Fig. 6. Although the behavior is generally similar to the propane and methane flames, there is a much larger scatter in the data. Indeed, it was observed that running the burner on butane yields flames that tend to flicker or are stable only at limited operating conditions. This is also evident from the recorded polarization curves that show non-linearities and strong scatter in particular at high v.

Within the parameter ranges investigated in the present study, we have observed a highest power density of $120\,\mathrm{mW\,cm^{-2}}$

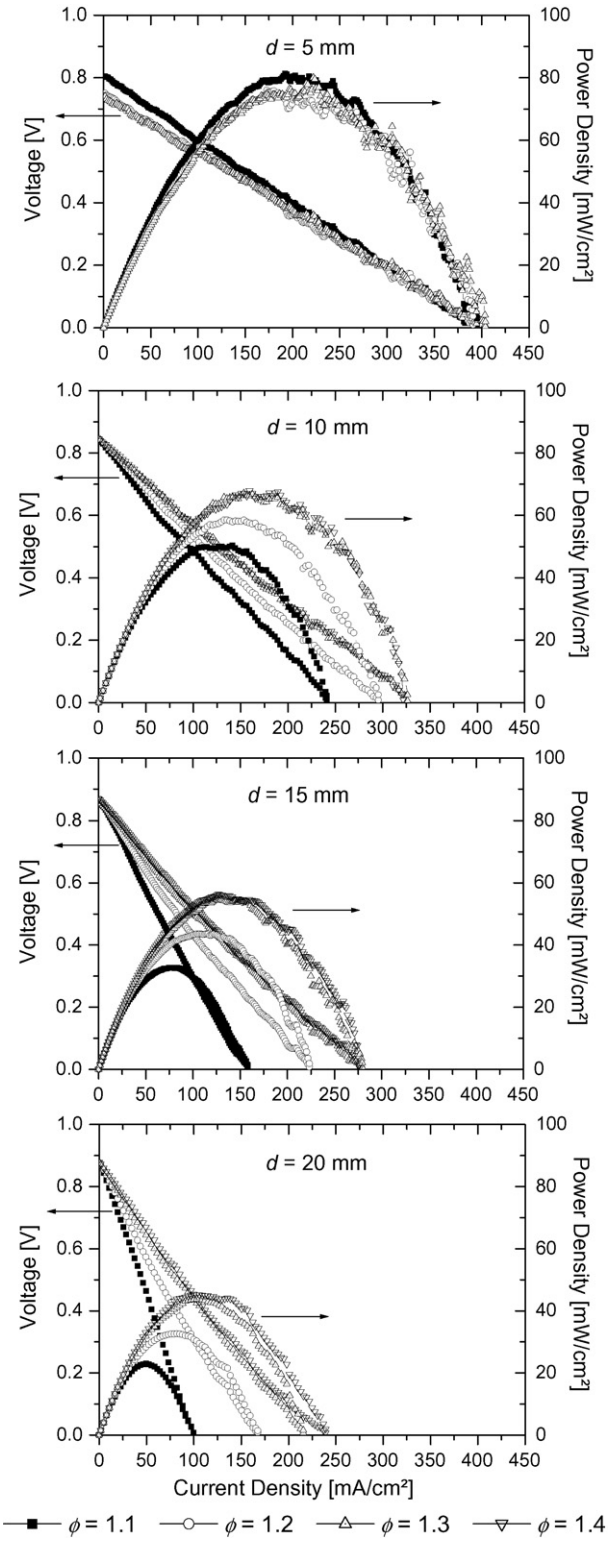

Fig. 3. Polarization curves of a DFFC system operated on methane for 20 cm s^{-1} gas inflow velocity and 5–20 mm distance from the burner (indicated in the figures) for equivalence ratios $\phi = 1.1$–1.4.

(propane/air, $\phi = 1.3$, $v = 30$ cm s^{-1}, and $d = 5$ mm). It should be noted that the goal of this study is not the maximization of power density, but the systematic study of the influence of flame operating conditions on fuel cell performance under defined operating

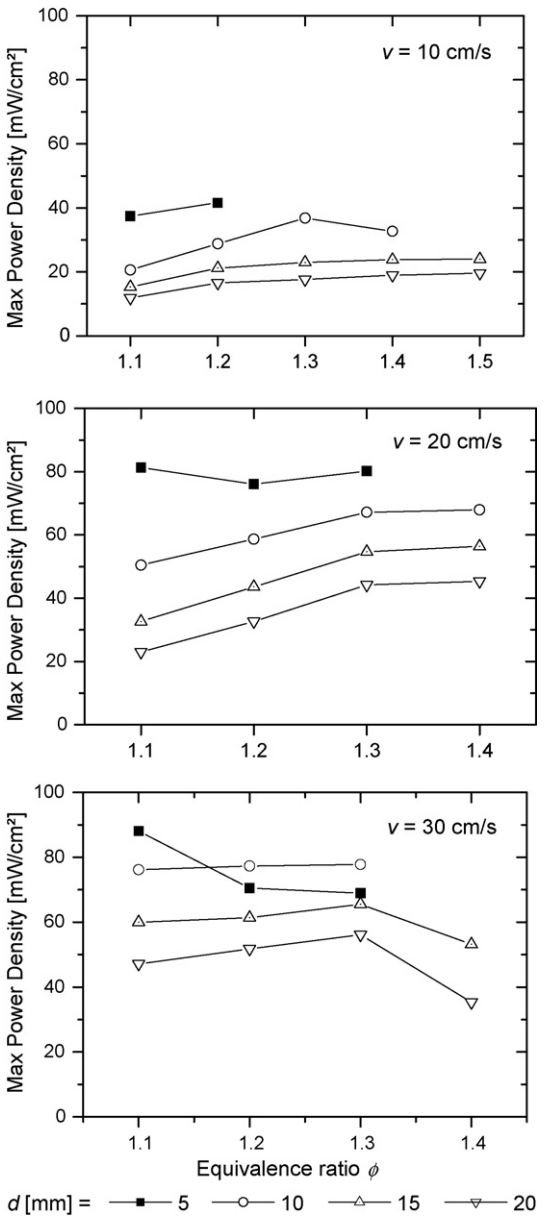

Fig. 4. *Methane-operated DFFC*: Maximum power density vs. equivalence ratio ϕ, distance between burner and SOFC d, and gas inlet velocity v.

conditions. For higher gas inflow velocities and thus increased fuel cell temperature power densities were observed to further increase.

3.3. Comparison of fuels

The maximum power density is plotted versus ϕ for all three fuels at $d = 10$ mm and $v = 20$ cm s^{-1} in Fig. 7. All fuels show a similar behavior, the maximum power density peaks at intermediate equivalence ratios ϕ. The power output is in general quite similar for all fuels. The methane flame yields slightly higher power densities in case of low equivalence ratios.

It should be noted that propane and butane flames can be operated over a wider range of equivalence ratios (up to $\phi = 1.9$) compared to methane flames (up to $\phi = 1.5$). No flame soot-

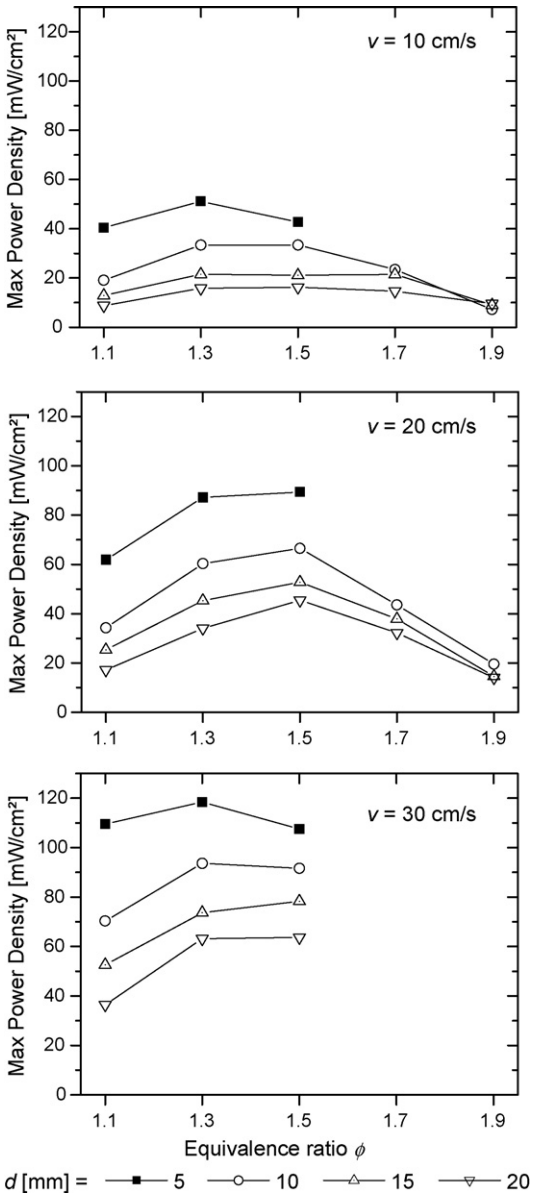

Fig. 5. *Propane-operated DFFC*: Maximum power density vs. equivalence ratio ϕ, distance between burner and SOFC d, and gas inlet velocity v.

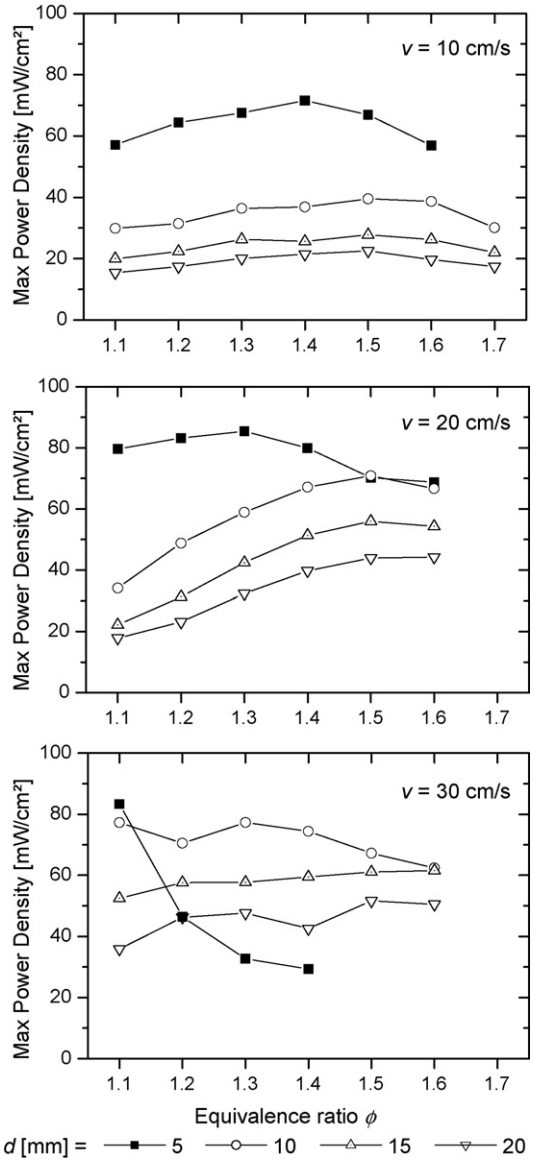

Fig. 6. *Butane-operated DFFC*: Maximum power density vs. equivalence ratio ϕ, distance between burner and SOFC d, and gas inlet velocity v.

ing was observed even at the highest equivalence ratios for the propane and butane flames, although these equivalence ratios are close to the flame sooting limits [17].

3.4. Temperature dependence of the power density

The temperature of the ceramic disc holder surface on the cathode side was measured using a thermocouple. For the various flame and fuel conditions investigated, it varies between 300 and 700 °C. The observed maximum power density is plotted versus the measured temperature in Fig. 8. Here, the upper panel (a) shows the collection of all data shown in Figs. 4–6, while the lower panel (b) shows data at one single value of the equivalence ratio ($\phi = 1.3$). In the latter case, all flames have approximately the same H_2 and CO concentrations in the exhaust gas.

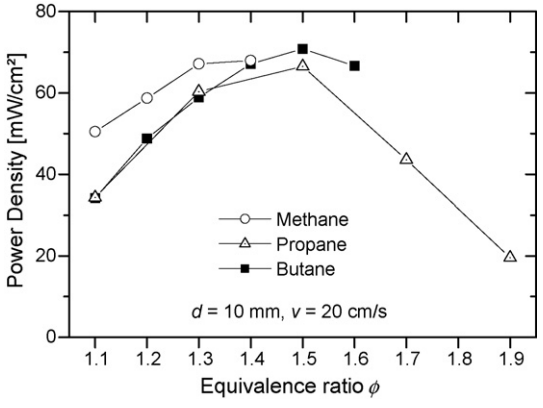

Fig. 7. Maximum power density vs. equivalence ratio ϕ for methane, propane, and butane operation at $d = 10$ mm and $v = 20\,\mathrm{cm\,s^{-1}}$.

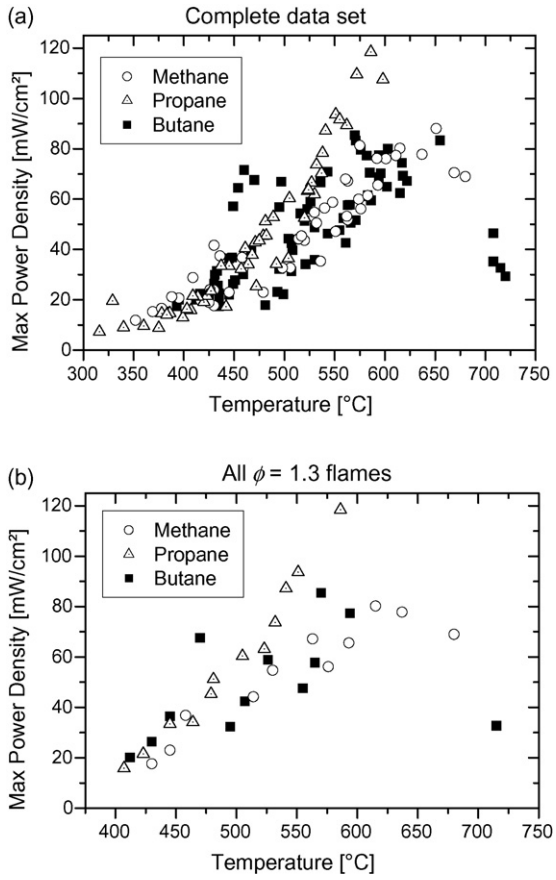

Fig. 8. Maximum power density vs. measured cell temperature for all methane, propane, and butane operating conditions.

The data shown in Fig. 8 reveal a strong correlation between the cell's maximum power density and its temperature. Indeed, the temperature dominates the influence of the other flame parameters, as the scatter in the data for one fixed temperature is smaller than the temperature dependence of the whole data set. The data also confirm that there is no systematic difference between the various fuels investigated; only the propane flames seem to have a slightly higher power output at high cell temperature. The scatter of the data shown in Fig. 8 is an indication of the instability of the flames. It is lowest for propane and increases for methane and butane. When comparing the data at a constant equivalence ratio (Fig. 8b), the propane flames show an almost linear relationship between power output and cell temperature.

There are several possible interpretations for the distinct temperature dependence of cell performance, including the temperature-dependent conductivity of the electrolyte, or the electrochemical kinetics of either cathode or anode. A more detailed analysis is subject of ongoing investigations.

The origin of the strong variation in cell temperature (300–700 °C) lies in the different flame configurations. In general, the only heat source within the DFFC system is the exothermic combustion chemistry that takes place in the thin (sub-mm) flame front. It leads to a heating of the gas-phase, and the SOFC is heated via conduction and convection from the gas-phase. The DFFC system loses heat via three mechanisms: (1) Heat conduction and convection away from the cathode surface; (2) heat conduction from the gas-phase to the cooled sinter plate of the burner, in particular at short distances between burner and SOFC; (3) radiation from both SOFC surfaces. Consequently, we observe that cell temperature (and therefore cell performance) increases with increasing gas inflow velocity (more overall flame heating power), decreasing distance between burner and SOFC (increased conductive heat transport towards SOFC), and decreasing equivalence ratio (stoichiometric or slightly rich flames are hottest).

3.5. The nature of the fuel for the solid oxide fuel cell

From detailed studies of flame structure and chemistry it is known [14,15,17] that the exhaust gases of rich ($\phi > 1.0$) premixed hydrocarbon/air flames consist of a mixture of mainly N_2, CO_2, H_2O, CO, and H_2, while molecular oxygen present in the fresh gases is consumed nearly quantitatively within the flame front. This is generally true for all kind of hydrocarbons, including alcohols, liquid, and solid fuels. For richer flames ($\phi \geq \sim 1.5$), methane may also be present in a percent range due to its thermodynamic stability. For sooting flames ($\phi \geq \phi_{\text{soot limit}}$, where $\phi_{\text{soot limit}}$ depends on fuel and flame configuration), higher hydrocarbons, polyaromatics, and soot (carbon) particles are present. As noted above, all flames investigated here were below the soot limit.

In order to assess the nature of fuel species available for the SOFC, calculations of the equilibrium gas composition and adiabatic flame temperature were performed for CH_4/air flames of various equivalence ratios $\phi = 0.8$–1.6. The upper value corresponds to the inflammability limit [18]. The simulations were carried out with the CANTERA software package [19] using thermodynamic data from the NIST-JANAF thermodynamical tables [20]. The resulting major species and temperature are shown in Fig. 9. The concentrations of both H_2 and CO increase for increasing equivalence ratio and reach values of to up to 10% for very rich flames. For lean flames ($\phi < 1.0$), excess O_2 is present, and H_2 and CO concentrations are very low. Temperature peaks close to stoichiometric conditions ($\phi = 1.05$) and decreases towards both lean and rich flames.

Given these observations, we believe that the chemical compounds that are available at the SOFC anode for conversion into electricity are both, H_2 and CO. The increase of fuel cell perfor-

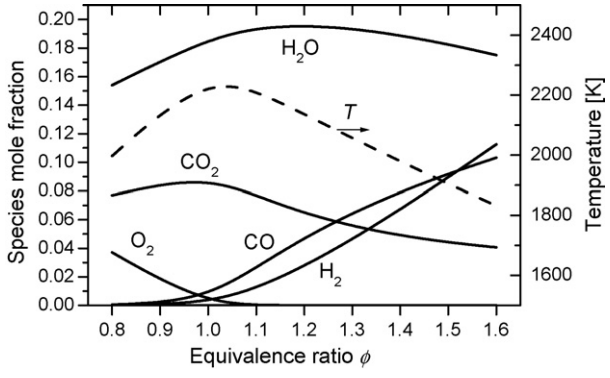

Fig. 9. Equilibrium calculations of major species concentrations and adiabatic temperature for CH_4/air flames of different equivalence ratios.

mance with increasing equivalence ratio (Fig. 4) is likely to be connected to the increase of the concentration of these species. At equivalence ratios $\phi \geq 1.5$ (Fig. 7), the decreasing flame temperature (Fig. 8) dominates the effect of further increasing H_2 and CO concentration. The type of fuel (methane, propane, and butane) has only a minor influence on cell performance because all fuels yield similar species concentrations in the exhaust gas.

The exhaust gas of stoichiometric and lean flames ($\phi \leq 1.0$) consists only of fully oxidized species (N_2, CO_2, and H_2O; excess O_2 for $\phi < 1.0$). This explains the observation that the DFFC system did not yield any electrical power when operated with stoichiometric or lean flames although the flame is hottest in this case: there is simply no fuel available for the fuel cell.

Near the hot flame front, radical species such as H, OH, and CHO can be present in the gas-phase in the percent range. However, closer to the anode surface, the radical concentration will strongly decrease to the order of parts per million. Although radicals may be highly reactive towards electrochemical oxidation, their low abundance most likely makes their contribution negligible.

These issues will be discussed in more detail, based on detailed combustion and electrochemistry simulations [3], in a future publication.

4. Conclusions

The direct-flame solid oxide fuel cell concept has a number of advantages over both dual-chamber and single-chamber SOFC systems, in particular its simplicity (no-chamber setup, no high-temperature sealing, and no external heater) and fuel flexibility (gaseous, liquid, and solid carbon-based fuels, low coking propensity). These properties make it an interesting candidate for energy conversion of hydrocarbon fuels, in particular for combined heat and power applications.

We have presented an experimental study of a DFFC operated with methane, propane, and butane fuels. A flat-flame burner provided a flame sheet parallel to and a few millimeters away from the anode surface. The results are summarized as follows.

- The flame operating conditions (equivalence ratio, gas inflow velocity, and distance between burner and fuel cell) have a strong influence on DFFC performance. This influence is quite complex, caused by the coupled flame chemistry, electrochemistry, and mass and heat transport. Within the parameter ranges investigated in the present setup, power densities of up to 120 mW cm^{-2} were achieved. Increasing the power output by choosing optimum burner type and flame conditions is subject of ongoing investigations.
- The choice of fuel itself (methane, propane, and butane) has only a minor influence on DFFC performance, as they are all converted to H_2/CO-rich exhaust gases in the flame. They have an indirect influence via the stability limits of the flame. With the present setup, propane flames were found most stable.
- Cell temperature has a dominant influence on the SOFC performance. In all experiments the correlation of power output with temperature is much stronger than with other parameters. The variation of cell temperature with flame operating conditions is a consequence of the coupled heat generation by combustion chemistry and heat losses by conduction and radiation.
- The fuel species available for the SOFC anode itself are both, H_2 and CO, that are produced by the fuel-rich flame (equivalence ratios $\phi > 1.0$). Increasing equivalence ratio causes an increase in these species concentrations, thus increasing cell performance. In the exhaust of stoichiometric or lean flames ($\phi \leq 1.0$), there is no H_2 or CO available, and the cell does not show any power output.

Given the observed increase of power density with temperature, we believe that optimizing thermal management (e.g. through thermal insulation) can lead to a further increase in cell performance. This should be true, in particular, for very rich flames where the effect of increasing H_2 and CO concentrations is so far compensated by a decreasing flame temperature.

References

[1] M. Horiuchi, S. Suganuma, M. Watanabe, J. Electrochem. Soc. 151 (2004) A1402–A1405.
[2] M. Horiuchi, S. Suganuma, M. Watanabe, Y. Tokutake, Proceedings of the Sixth European Solid Oxide Fuel Cell Forum, Lucerne, Switzerland, 2004, pp. 154–162.
[3] H. Kronemayer, W.G. Bessler, M. Vogler, M. Horiuchi, S. Suganuma, Y. Tokutake, C. Schulz, J. Warnatz, Proceedings of the Seventh European Solid Oxide Fuel Cell Forum, Lucerne, Switzerland, 2006.
[4] T. Hibino, H. Atsuko, I. Takao, T. Jun-ichi, Y. Shin-ichiro, S. Mitsuro, Science 288 (2000) 2031–2033.
[5] Z. Shao, S.M. Haile, J. Ahn, P.D. Ronney, Z. Zhan, S.A. Barnett, Nature 435 (2005) 795–798.
[6] T.W. Napporn, X. Jacques-Bédard, F. Morin, M. Meunier, J. Electrochem. Soc. 151 (2004) A2088–A2094.
[7] P. Jansinki, T. Suzuki, F. Dogan, H.U. Anderson, Solid State Ionics 175 (2004) 35–38.
[8] Y. Hao, Z. Shao, J. Mederos, W. Lai, D.G. Goodwin, S.M. Haile, Solid State Ionics 177 (2006) 2013–2021.
[9] J.P. Bingue, A.V. Saveliev, A.A. Fridman, L.A. Kennedy, Int. J. Hydrogen Energy 27 (2002) 643–649.
[10] H. Pedersen-Mjaanes, L. Chan, E. Mastorakos, Int. J. Hydrogen Energy 30 (2005) 579–592.
[11] R.S. Dhamrat, J.L. Ellzey, Combust. Flame 144 (2006) 698–709.
[12] K. Kendall, C.M. Finnerty, J.C. Austin, T. Alston, J. Mater. Sci. 36 (2001) 1119–1124.
[13] C.M. Finnerty, G.A. Tompsett, K. Kendall, R.M. Ormerod, J. Power Sources 6 (2000) 459–463.
[14] R.J. Kee, M.E. Coltrin, P. Glarborg, Chemically Reacting Flow. Theory and Practice, John Wiley & Sons, 2003.
[15] J. Warnatz, U. Maas, R.W. Dibble, Combustion, third ed., Springer, Heidelberg, 2001.
[16] M. Gödickemeier, L.J. Gauckler, J. Electrochem. Soc. 145 (1998) 414–421.
[17] I. Glassman, Combustion, third ed., Academic Press, San Diego–London–Boston–New York–Sydney–Tokyo–Toronto, 1996.
[18] R.C. Weast, M.J. Astle (Eds.), CRC Handbook of Chemistry and Physics, 63 ed., CRC Press, Boca Raton, Florida, 1982.
[19] D.G. Goodwin, Cantera, http://www.cantera.org, 2001–2005.
[20] M.W. Chase, C.A. Davies, J.R. Downey, D.J. Frurip, R.A. McDonald, A.N. Syverud, J. Phys. Chem. Ref. Data 14 (Suppl. 1) (1985).